CERENKOV DETECTORS IN THE ALPHA MAGNETIC SPECTROMETER

F. BARAO
LIP, Av. Elias Garcia, 14, 1
1000-Lisboa, Portugal
e-mail: fernando.barao@cern.ch

Cerenkov detectors have been widely used in High Energy Physics and Astrophysics. Their use allows to measure the velocity and charge magnitude of charged particles in a very accurate way, leading to particle identification. The Alpha Magnetic Spectrometer (AMS) whose test flight took place last June 1998, was equipped with an Aerogel Threshold Counter mainly for antiproton identification purposes. Additionally, the counter was also used to improve the selection of positrons. In a second phase, the AMS spectrometer capabilities will be extended through the inclusion of a Ring Imaging Cerenkov detector (RICH).

1 Introduction

The Cerenkov radiation effect was fully characterized in 1934 by Vavilov and Cerenkov and later on explained in terms of classical electromagnetic theory by Tamm and Frank [1]. It consists on the existence of electromagnetic radiation emitted by a charged particle when this one acrosses a dielectric medium with a velocity larger than the light velocity in that medium. The emission angle (Cerenkov angle θ_c) depends on the particle velocity ($\beta \equiv v/c$) and on the medium refractive index (n),

$$cos\theta_c = \frac{1}{\beta n} \tag{1}$$

Figure 1 shows the Cerenkov angle dependence in terms of the particle relative velocity and for different refractive index values. It can be figured out that the Cerenkov angle increases with the the particle velocity and medium refractive index. The maximum Cerenkov angles ($\beta = 1$) range from about 15 degrees up to 45 degrees for materials having refractive indexes between 1.05 and 1.4, typically aerogel and liquid/solids materials.

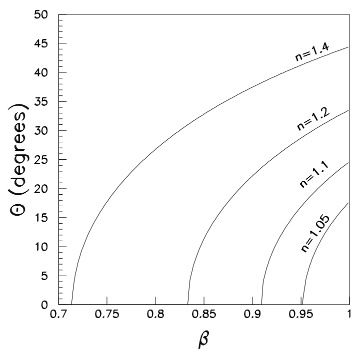

Figure 1. Cerenkov angle dependence as function of particle velocity and refractive index.

From equation (1) it follows that only particles with velocities above a threshold $\beta_t > 1/n$ will emit photons. Thus, the threshold energy for a certain particle of mass *m* is defined as,

$$E_t = m\frac{n}{\sqrt{n^2-1}} \tag{2}$$

The number of radiated photons per unit of length and energy is given by [1],

$$\frac{d^2N}{dxdE} = \left(\frac{2\pi\alpha}{hc}\right) Z^2 sin^2\theta_c = \left(\frac{2\pi\alpha}{hc}\right) Z^2 \left(1 - \frac{1}{\beta^2 n^2}\right) \tag{3}$$

Therefore, the light yield increases with the radiator thickness (L), the particle charge (Z), the particle velocity (β) and the refractive index of the medium (n). The photons are emitted uniformly along the path of the particle in the radiator and their wavelength (λ) distribution follows a $1/\lambda^2$ dependence.

The constant term on expression (3) can be calculated as $370\ cm^{-1}eV^{-1}$. The total number of photons emitted in a radiator of thickness L can be obtained by integrating equation (3). Taking into account the overall efficiency (ε) for detecting the emitted photons which includes the effects of their propagation up to the arrival into the photodetectors (collection efficiency) and the detection efficiency (quantum efficiency) of the devices, the number of photoelectrons per unit of length (cm) is,

$$N_{p.e} \simeq 370\ L < sin^2\theta_c > \int \varepsilon(E)dE \tag{4}$$

The choice of the radiator medium imposes clearly the magnitude of the detector output response. For the two extreme mediums showed in figurea factor 6 on the $N_{p.e}$ output ratio is obtained.

2 Astrophysics motivations

Cerenkov detectors have been widely used in Astrophysics for particle identification purposes namely in balloon experiments like BESS [2], CAPRICE [3], ISOMAX [5] and others. Besides the velocity measurement they can be very useful to reject albedo particles and for element separation ($N_{p.e} \propto Z^2$). Antiproton identification and isotope separation are major physics topics where the Cerenkov detectors can contribute due to the excellent resolution provided on $\Delta\beta/\beta$. Moreover, in the case of directional Cerenkov detectors where only downward particles can trigger, the apparatus sensitivity for antimatter search is improved.

Search for antimatter is one of the physics goals of the Alpha Magnetic Spectrometer. Since the Universe at the beginning was symmetric, the question to answer in the framework of a symmetric universe is at which scale this symmetry exists. Absence of γ radiation from antimatter annihilation ruled out domains of matter-antimatter within ~ 20 Mpc, typically the size of galactic clusters [11]. Therefore, the existence of conglomerates of antimatter at scales larger than clusters of galaxies has not yet been excluded by present observations. A direct indication of antimatter would be the detection of antinuclei since its secondary production is very hard. The current sensitivity on the search for antihelium is at 10^{-6} level [12].

Antiprotons are part of the cosmic rays arriving at earth. Their existence was revealed in 1979 [6] and since then many measurements were performed. The production of antiprotons is supposed to occur through collisions between primary cosmic rays, essentially protons, and the interstellar medium. Its study is important to understand the propagation of cosmic rays namely of its major proton component and it can provide evidence for the presence of primary Exotic Sources like Dark Matter [7] and primordial black holes [8]. An eventual signal of primary antimatter must be searched for in the low energy region of the antiproton spectrum where the secondary component steeply decreases.

Element isotopes of secondary origin is another component of charged particles reaching earth and can provide us with information about propagation, time confinement and the origin of cosmic rays. The study of the abundance of ^3He, which is rare in nature ($\sim 10^{-4}$) and is likely produced by collisions of ^4He with the interstellar medium, constrain models of cosmic ray propagation. Recent data results were published [9] by the IMAX [4] experiment up to around 3.5 GeV/nucleon kinetic energy. Similarly, Deuterium-Hydrogen ratio ($< 10\%$) can be used to monitorize the proton propagation and source spectrum.

Radioactive nuclides having decay times of the order of propagation timescales provide a way of determining the confinement time of the cosmic rays and the average density found on their transport. The abundance of the beryllium isotope ^{10}Be with a half-life time of 1.6×10^6 years was measured by different spacecraft experiments [10]. The confinement time of cosmic rays derived was $\sim 10 - 30$ Myears and the average density crossed $\sim 0.2 - 0.3$ H atoms/cm^3 [10]. The density of matter found is lower than the 1 $atom/cm^3$ normally associated to the galactic disk. This can suggest that the cosmic rays spend a large fraction of their time in low density regions (galactic halo).

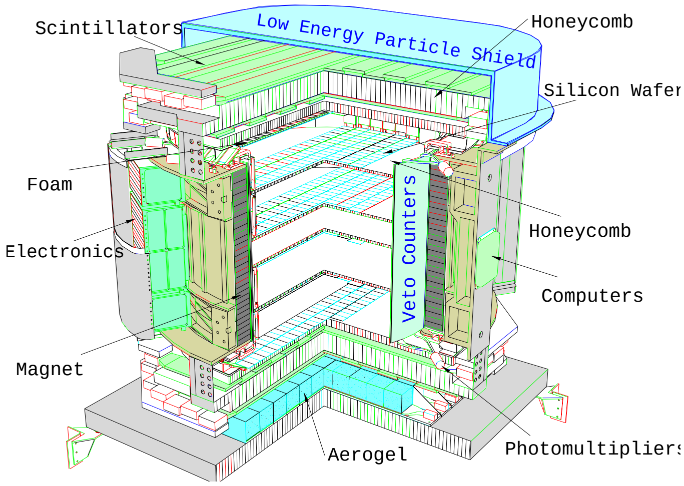

Figure 2. Scheme of the AMS detector sent to a ten days flight during June 1998.

3 AMS/I: the aerogel Cerenkov counter

AMS (Alpha Magnetic Spectrometer) [13] is a detector apparatus designed to search for antimatter, matter and missing matter. The first phase of the AMS experiment was achieved on board of the Space Shuttle Discovery, during a ten days flight in June 1998. The experiment flew in an orbit 51.6 degrees inclined and at an mean altitude of 370 Km. The AMS data acquisition system lifetimes varied between 40 and 95%, with recorded event rates of 700 to 100 Hz. A total number of 99 million events were accumulated. This experimental flight had an apparatus composed of a permanent magnet, a time-of-flight system (TOF), a silicon tracker (TRK), veto counters and an Aerogel Threshold Counter (ATC). The main idea was to submit the experiment to the conditions it has to support to be placed and remain for three years on the International Space Station (ISSA). Additionally and given the scanning on latitude-longitude performed by the Shuttle, the data taken can be explored to measure the particle fluxes at different geomagnetic positions and increase the world statistics on antiprotons.

The antiprotons analysis has to deal with an electron background whose expected ratio is $e/\overline{p} \sim 10^2$. The ATC main purpose was to extend the proton/electron separation up to higher momenta. Thus, an aerogel radiator with a refractive index of 1.036 [14] was chosen leading to an antiproton momentum threshold of 3.5 GeV/c. Therefore, the antiproton-electron separation relies on the fact that up to the threshold momentum an electron has a maximum cerenkov signal ($\beta \sim 1$) whereas an antiproton presents no signal.

The ATC is made of 11 modules superimposed in two layers of 5 and 6 modules, respectively from top to bottom. The first layer was placed 10 cm below the last TOF scintillator plane and the two layers were separated by a distance of 20 cm. Every module, excepting the half-module placed on the border of bottom layer, is composed of 16 aerogel cells ranged in two columns of cells with a size of $11 \times 11 \times 9\ cm^3$. The propagation of photons on the aerogel is affected by two effects, the Rayleigh scattering ($L_{int}^{sca} \propto \lambda^4$) and the absorption ($L_{int}^{abs} \propto \lambda^2$). In order to minimize the importance of both effects in the photon collection efficiency, a layer of wavelength shifter was placed in the middle of the cell. It is made of PMP dispersed in a tedlar foil ($25\ \mu m$) and enveloped with poliethilene ($50\ \mu m$) to avoid the contact with the aerogel. The PMP (1-phenyl 3-mesityl-pyrazoline) shifts the wavelength of the photons to higher values, peaking at 420 nm. The cerenkov light emitted and diffused in the aerogel is reflected in the cell walls by three teflon foils $250\ \mu m$ thick and is detected in a photomultiplier tube (PMT) Hamamatsu R59000 located at the bottom of the cell. To insure the opacity of every cell, the cell walls were covered with a mylar foil.

The ATC geometrical acceptance when both layers are required to be crossed is around 70% of the tracker acceptance. A number of 3.5 photoelectrons on the upper layer and 4.0 on the lower layer was detected for particles having $\beta = 1$. Figure 3 shows the detector signal response for protons, integrated for the two layers, as function of momentum. Three regions can be distinguished. Above threshold ($\sim$ 3.5 GeV/c) the signal follows the expected Cerenkov momentum dependence where $N_{p.e} \propto (1 + (m/p)^2)$. Below threshold, the contribution from residual signals due to scintillation, $\delta - rays$, Cerenkov effect in the wavelength shifter and direct PMT Cerenkov radiation is visible and was estimated in average as 0.5 photoelectrons per cell.

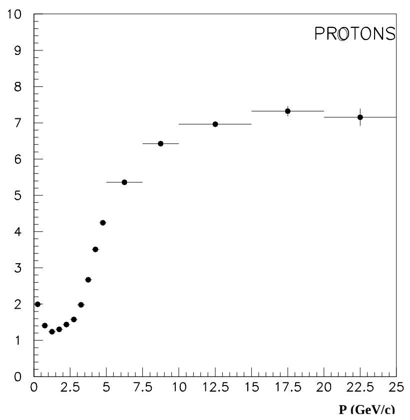

Figure 3. The ATC response for protons.

For very low momenta (< 0.5 GeV/c) the signal response increases, following the rise on the scintillation energy deposited by low beta protons ($dE/dx \propto \beta^{5/3}$). The detector calibration was performed on a cell by cell basis by measuring the single photoelectron peak due to the residual light deposited in the detector by below threshold protons.

The antiproton selection efficiency obtained with the ATC by is around 50% at 1 GeV/c and decreases to 40% for antiprotons with 3 GeV/c. The rejection power against electrons was estimated as around 300 [15].

ATC can also be used to distinguish positrons from protons where a large unbalanced signal to contamination ratio is expected ($e^+/p \sim 10^{-3}$). Positrons are expected to leave a maximum signal on every detector layer whereas protons below threshold will contaminate the e^+ sample due to the residual signal effects explained before. Furthermore these physical signals can be artificially stressed by after-pulses effects present on the PMTs. A selection efficiency of 45% for positrons was calculated by imposing independent signal cuts (2 p.e) on every layer. The proton rejection imposed by the ATC depends on the proton momentum and ranges from 150 to 50 for momenta from 1 to 3 GeV/c.

4 AMS/II: the RICH option

The AMS phase II will include new detector systems such as an Electromagnetic Calorimeter, a Transition Radiation Detector (TRD) and a Ring Imaging Cerenkov detector (RICH).

The RICH [16,17] will contribute to the achievement of the AMS physics prospects namely on the following points:

- the search for antimatter with a sensitivity of 10^{-9} will benefit from the high rejection efficiency against albedo particles provided by the RICH.

- the search for missing matter will imply the selection of antiprotons and positrons samples with high purity in an momentum range as large as possible.

- the astrophysics studies on the cosmic ray propagation and confinement time will require accurate measurements of the ratios of secondary isotopes and will benefit from the extension of these results as far as possible in momentum.

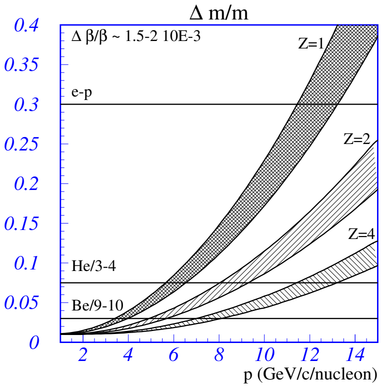

Figure 4. Mass resolution as function of momentum per nucleon.

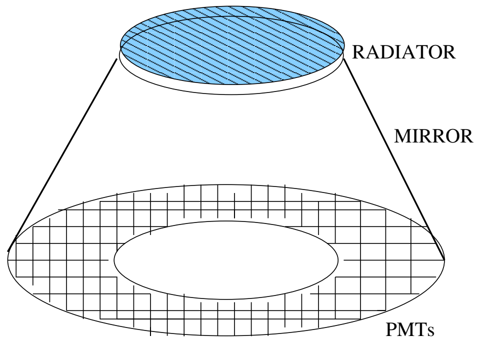

Figure 5. RICH schematic view for AMS phase II.

Particle identification requires the velocity (β) measurement by the RICH and the momentum (p) measurement from tracker. The particle mass is obtained with,

$$m = p\sqrt{\frac{1}{\beta^2} - 1} \tag{5}$$

The associated mass uncertainty depends on both the momentum and velocity accuracies,

$$\frac{\Delta m}{m} = \frac{\Delta p}{p} \oplus \gamma^2 \frac{\Delta \beta}{\beta} \tag{6}$$

where $\gamma = E/m$ is the Lorentz factor. From equation (6) it is clear that the error on the velocity will dominate as the momentum increases. The error on the velocity determination depends on how accurate the Cerenkov angle (θ_c) is reconstructed and both uncertainties are related through,

$$\frac{\Delta \beta}{\beta} = tan\theta_c \Delta\theta_c \tag{7}$$

The uncertainty on β scales down by a factor $1/\sqrt{N}$, where N is the number of photons detected. Other error sources are the radiator thickness, the pixel size of the photodetectors and the dependence of the refractive index on the photon energy (chromaticity error).

The RICH will make a velocity measurement with a resolution $\Delta\beta/\beta \sim 10^{-3}$. Figure 4 shows the typical mass accuracy as function of the particle momentum per nucleon, obtained for a velocity measured with an accuracy between 0.15% and 0.2%. It has been assumed a momentum resolution of 1% up to 10 GeV/c with a degradation to 3% at around 100 GeV/c. Requiring a 3σ separation and assuming for simplicity balanced fluxes, one can roughly estimate the momentum regions where the element separation can be achieved. Thus, electron-proton can be distinguished up to $\sim 10{-}12\, GeV/c$ whereas ^3He- ^4He and ^{10}Be- ^9Be can be separated up to $\sim 7-8\; GeV/c/amu$.

The RICH in AMS will be located just after the Tracker and Time-of-Flight and before the Electromagnetic Calorimeter. A schematic view of the RICH detector can be seen on figure 5. A major constrain to the RICH design was to have a minor contribution to the amount of matter traversed by the cosmic rays and to be in a region of a manageable magnetic field. Therefore, the detection plane (PMTs) was placed in the bottom of the detector where the magnetic field is weaker ($B \sim 250$ G). The central region, corresponding to the ECAL acceptance, was not equipped with photodetectors. The RICH geometry will be conical shaped with a radius on the top of 65 to 70cm, a height of 50 cm and a bottom radius close to 80 cm. The solid radiator, made of Sodium Fluoride (NaF) or Aerogel, will be located on the top of the RICH and will be 1 to 2 cm thick. The Aerogel has a lower refractive index thus favoring particle identification on higher momentum ranges but its clarity can be critical as scattered photons constitute a background to the Cerenkov angle reconstruction. Photomultipliers providing a 4x4mm pixel size are currently assumed to be the photodetectors candidates but 8X8cm pixelization is being studied. As these devices are sensitive to the magnetic field a magnetic shielding has to be included. The number of photomultipliers to be used is around 1200. Light collectors will be coupled to the photodetectors in order to increase the light collection efficiency.

5 Conclusions

After the successful experimental flight of the AMS experiment on June 1998 aboard of Space Shuttle Discovery, the AMS capabilities will be improved and extended. In particular, the physics prospects envisaged by the Cerenkov Threshold Counter during the first flight can be significantly improved and extended with a RICH detector. The RICH, a proximity focusing device, must be able to perform electron-proton separation up to 10 GeV/c. Moreover, it will be a key instrument for the isotopes physics analysis and by the addition will improve the AMS capability for albedo rejection.

Acknowledgments

I would like to thank Peter Fisher and Giuliano Laurenti for the many discussions we had on the RICH topic for AMS. My thanks go also to Jean Favier and Roman Kossakowski for the collaboration on the ATC and William Burger for reading part of this manuscript. Many thanks to the Conference Organizers for the pleasant stay.

References

1. T. Ypsilantis and J. Seguinot, *Nucl. Instrum. Methods* A **343**, 30 (1994). See references therein.
2. K. Yoshimura et al., *Phys. Rev. Lett.* **75**, 3792 (1995).
   Y. Asaoka et al., *Nucl. Instrum. Methods* A **416**, 236 (1998).
3. R. L. Golden, *Proposal to NASA*, NRA-92 OSSA-10.
   G. Barbiellini et al., *Nucl. Instrum. Methods* A **371**, 169 (1996).
4. J. W. Mitchell et al., *Proc. 23rd Int. Cosmic Ray Conf.*, 1, 519 (1993).
5. J. W. Mitchell et al., *Proc. 26th Int. Cosmic Ray Conf.*, 3, 113 (1999).
6. R. L. Golden, *Phys. Rev. Lett.* **43**, 1196 (1979).
7. J. Silk, *Phys. Rev. Lett.* **53**, 624 (1984).
8. J. H. MacGibbon, *Astrophys. J.* **371**, 447 (1991).
9. O. Reimer, *Astrophys. J.* **496**, 490 (1998).
10. J. J. Connell, *Astrophys. J.* **501**, L59 (1998).
11. A. G. Cohen et al., *Astrophys. J.* **495**, 539 (1998).
12. T. Saeki et al., *Phys. Lett.* B **422**, 319 (1998).
13. S. P. Ahlen et al., *Nucl. Instrum. Methods* A **350**, 34 (1994).
    V. M. Balebanov et al., *AMS proposal to DOE*, approved April 1995.
14. A. K. Gougas et al., *Nucl. Instrum. Methods* A **421**, 249 (1999).
15. F. Barao et al., *Analysis of the Aerogel Threshold Cerenkov data from AMS flight (STS-91)*, AMS-note 99-38 (1999).
16. P. Fisher, *AMS RICH design notes*, AMS internal note (1998).
17. A. Barrau et al., *Proposal for the RICH counter of AMS on the International Space Station*, AMS internal report (1998).